J Mater Sci: Mater Med (2008) 19:1839–1850
DOI 10.1007/s10856-008-3384-7

Surface modifications of silicon nitride for cellular biosensor applications

Johan Gustavsson · George Altankov · Abdelhamid Errachid · Josep Samitier · Josep A. Planell · Elisabeth Engel

Received: 2 May 2007 / Accepted: 28 December 2007 / Published online: 25 January 2008

Abstract Thin films of silicon nitride (Si_3N_4) can be used in several kinds of micro-sized biosensors as a material to monitor fine environmental changes related to the process of bone formation in vitro. We found however that Si_3N_4 does not provide optimal conditions for osseointegration as osteoblast-like MG-63 cells tend to detach from the surface when cultured over confluence. Therefore Si_3N_4 was modified with self-assembled monolayers bearing functional end groups of primary amine (NH_2) and carboxyl (COOH) respectively. Both these modifications enhanced the interaction with confluent cell layers and thus improve osseointegration over Si_3N_4. Furthermore it was observed that the NH_2 functionality increased the adsorption of fibronectin (FN), promoted cell proliferation, but delayed the differentiation. We also studied the fate of pre-adsorbed and secreted FN from cells to learn more about the impact of above functionalities for the development of provisional extracellular matrix on materials interface. Taken together our data supports that Si_3N_4 has low tissue integration but good cellular biocompatibility and thus is appropriate in cellular biosensor applications such as the ion-sensitive field effect transistor (ISFET). COOH and NH_2 chemistries generally improve the interfacial tissue interaction with the sensor and they are therefore suitable substrates for monitoring cellular growth or matrix deposition using electrical impedance spectroscopy.

J. Gustavsson · J. A. Planell · E. Engel (✉)
Biomaterials, Biomechanics and Tissue Engineering Group, Department of Materials Science and Metallurgy, Universitat Politècnica de Catalunya, Avda. Diagonal 647, Barcelona 08028, Spain
e-mail: Elisabeth.Engel@upc.edu

G. Altankov
ICREA – Institució Catalana de Recerca i Estudis Avançats, Barcelona, Spain

G. Altankov · A. Errachid · J. Samitier · J. A. Planell
Laboratory of Nanobioengineering, Institut de Bioenginyeria de Catalunya, Parc Científic de Barcelona, C/Josep Samitier 1-5, Barcelona 08028, Spain

A. Errachid · J. Samitier
Department of Electronics, Universitat de Barcelona, Martí i Franquès 1, Planta 2, Barcelona 08028, Spain

1 Introduction

As a ceramic, silicon nitride (Si_3N_4) is considered as a biocompatible material in contact with bone in vitro [1, 2] and has been suggested as a load-bearing implant material due to its favourable mechanical properties [3]. In a different material configuration, namely as a low pressure chemically vapour deposited (LPCVD) thin film, Si_3N_4 can also be used as the sensitive material in miniaturized biosensors such as the *ion-selective field effect transistor* (ISFET) [4] or the *electrolyte/insulator/semiconductor* microtransducer [5]. Such devices can for example be used to obtain information about cell metabolic activity based on pH measurements [6, 7]. Besides being sensitive to hydrogen ions Si_3N_4 insulating substrates are also used in other ion sensitive applications after adhesion of additional films that allow for good selectivity and high sensitivity [8]. It is further proposed that Si_3N_4 can be a suitable sensing material for quantification of antigen–antibody reactions through specific surface modifications [9] and for monitoring cell growth using electrical impedance spectroscopy (EIS) techniques. Considering all the above applications of Si_3N_4 as sensor material for monitoring bone formation in vitro, we have initiated broad-spectrum

studies on its cellular biocompatibility to learn how it will affect the functional behaviour of osteoblast-like cells.

In vitro cytotoxicity evaluations [10] and in vivo studies [11, 12] generally have classified LPCVD Si_3N_4 as a biocompatible material. When Si_3N_4 was compared to other silicon thin films regarding fibroblast response it was shown that Si_3N_4 supported well both protein adsorption and cell proliferation [13]. In our own study we found, however, that Si_3N_4 does not provide optimal conditions for osseointegration as osteoblast-like cells detached from the surface when cultured over confluence. Furthermore it is known that integration of biosensors in a surrounding biological entity leads to biofouling with proteins and cells adhering to the surface [14, 15], and as a result the sensor signal is impeded. An important issue of biofouling is the fate of adsorbed matrix proteins such as fibronectin (FN), vitronectin, and fibrinogen which often behave rather complex on biomaterial surfaces. Particularly for FN, which is the main adhesive protein responsible for cell–biomaterials interaction [16, 17], there is a line of investigations showing that adsorbed FN is actively removed and reorganised by adhering cells. This is presumably a process that reflects the ability of adhering cells to form extracellular matrix on biomaterials interface [17–19], and indeed could alter the biosensor performance. Thus it becomes clear that the adsorption of protein, its fate, and the subsequent cellular interaction with Si_3N_4 need to be carefully controlled and better understood for specific biosensor applications.

Self assembled monolayers (SAMs) have been successfully used to tailor material surface properties to obtain control over the cellular responses [20, 21]. In this study two different organosilanes bearing functional end groups of primary amine (NH_2) and carboxyl (COOH) respectively were tailored to the bare Si_3N_4. These modifications provide different physicochemical properties such as wettability and surface charge. Moreover, both the NH_2 and the COOH can be used for further surface modifications connected to biosensor applications [9, 22] while they at the same time are functional groups uniformly available in nature. We could show here that NH_2 and COOH effectively can guide the interaction of osteblast-like MG-63 cells. Specifically we investigated the initial cell adhesion and spreading, cell proliferation and differentiation, where the levels of alkaline phosphatase activity and osteocalcin production were used as indicators of bone turnover. The fate of adsorbed and secreted fibronectin, which undergo significant remodelling by adhering MG-63 cells, was also studied in an attempt to understand the impact of above functionalities for the osseointegration, a process that relate to the development of provisional extracellular matrix on biomaterials interface. Details of this investigation are presented herein.

2 Materials

2.1 Silicon nitride samples

Squared sized samples of 10 mm^2 were cut from a P-type <100> silicon wafer that had been exposed to low pressure chemical vapour deposition (LPCVD) to obtain layers of 300 Å silicon dioxide (SiO_2) and 500 Å Si_3N_4 respectively. Such a sandwich structure of Si–SiO_2–Si_3N_4 resembles the build up of a typical H^+-sensitive ISFET gate region.

2.2 Self-assembled monolayers

Two different SAMs were prepared according to previously described protocols [23, 24] utilizing organosilanes 3-(2-aminoethylamino)propyltrimethoxysilane (Fluka; $C_8H_{22}N_2O_3Si$; functional group of NH_2), and 10-(Carbomethoxy)decyl dimethylchlorosilane (ABCR GmbH & Co; $C_{14}H_{29}ClO_2Si$; to give functional group of COOH after activation with HCl). From here on, each SAM is referred to as its functional end group (i.e., NH_2 or COOH respectively).

In brief, before performing aqueous silanisation of the Si_3N_4 samples they were pre-cleaned in an ultrasonic bath for 10 min in a 1:1 mixture of 2-propanol and tetrahydrofuran, and then dried under argon (Ar) flow. The samples were then exposed to a piranha solution of 30% (v/v) H_2O_2 with 70% (v/v) H_2SO_4 for 30 min followed by a copious rinse with distilled water (18.2 MΩ). To perform the NH_2 silanisation the samples were placed in a solution containing 30 ml methanol and 10 ml of 4% acetic acid glacial, finally adding the $C_8H_{22}N_2O_3Si$ to yield a 1% solution. The samples were left in this solution for 18 min at room temperature. Excess silane was washed away by moving the samples to a silane-free solvent solution formulated as above, before dried and cured during one hour at 80°C. To obtain COOH samples, the cleaned samples were carefully dried under Ar flow and then immersed in a 0.010 M solution of $C_{14}H_{29}ClO_2Si$ for 4 h at 4°C in a 1:3 mixture of CCl_4 and n-C_7H_{16}. After washing away the excess silane, and after curing it as above, the COOH samples were immersed overnight in 12 M HCl.

2.3 Contact angle measurements

Water contact angle measurements were used to estimate the wettability of the involved surface chemistries. The advancing and receding contact angles of a drop of distilled water (3 µl) on the solid substrates were measured in air and at room temperature with the sessile contact angle

method (Dataphysics Contact Angle Systems OCA15). Average values were obtained from at least ten samples.

2.4 Preparation of FITC-labelled fibronectin

Human plasma fibronectin (FN) (Sigma) was dissolved in 0.1 M sodium bicarbonate buffer (pH = 9.0) at 1 mg/ml. Then 10 µl of fluorescein isotiocianate (FITC; Sigma) dissolved in dimethylsulfoxide to 10 mg/ml was added and left for 2 h at room temperature. The labelled FN was separated from non-conjugated dye on a Sephadex G-25 desalting column equilibrated with phosphate buffered saline (PBS) solution. The final protein concentration was estimated by measuring the absorbance at 280 nm, while the degree of FITC-labelling was calculated against the absorbance at 494 nm. The samples were stored at 4°C.

2.5 Adsorption of FITC-labelled fibronectin

Quantitative information on FN adsorption was obtained as has been described elsewhere [25, 26] by dissolving pre-adsorbed FITC-labelled FN from the sample with NaOH and then measuring its fluorescent intensity. Briefly, each sample was ultrasonically cleaned in ethanol and distilled water respectively for 10 min before dried under Ar flow. The samples were then coated with 100 µl of FITC-labelled FN (20 µg/ml) and incubated for 30 min at 37°C. After rinsing twice with PBS the samples were exposed to 0.5 ml of 0.2 M NaOH for 2 h at room temperature. The fluorescent intensity of the dissolved FITC-FN was measured with a fluorospectrophotometer (Shimadzu) set to 488 nm (excitation) and 530 nm (emission) and compared to a standard curve based on known concentrations of fresh FITC-FN solutions in 0.2 M NaOH.

2.6 Cell culture

The human osteoblast-like MG-63 cell line (purchased from ATCC) was used as model to examine the effects of surface chemistry on osteoblast adhesion, proliferation, differentiation, and FN reorganisation. Cells were maintained in Dulbeccós modified Eagle medium supplemented with 10% fetal bovine serum (FBS), 1% penicillin/streptomycin, 2 mM L-glutamine, and 1 mM sodium pyruvate, in a humidified atmosphere of 5% CO_2 in air. The culture medium was exchanged every second day and upon confluence the cells were detached with a minimum amount of trypsin-EDTA that was inactivated with FBS after 5 min. The cells were then either re-cultured or used for experiments.

For cell experiments, Si_3N_4 and SAMs substrates were sterilised in 70% ethanol during 10 min, and then copiously rinsed with sterile PBS. The samples were individually placed in tissue culture plates (Nunc) with a culture area of 1.9 cm^2.

2.6.1 *Initial cellular interactions*

To investigate initial cell adhesion and morphology 2.0×10^4 cells/well were seeded to each surface chemistry in 2.0 ml serum free medium. One set of samples had been pre-coated with FN (20 µg/ml) for 30 min at 37°C. After 2 h of incubation, the living cells were stained with 0.001% fluorescein diacetate (FDA) dissolved in acetone. Under these conditions the vital cells convert FDA in a fluorescent analogue via their esterases and could be viewed on an inverted fluorescent microscope (Nikon, Eclipse E600). Representative pictures of the adhered cells were then taken using the green channel of the fluorescent microscope. Morphological parameters such as the *area* and the *perimeter* were evaluated using automated image analysis software (analySIS 3.00, Soft Imaging System GmbH). The *roundness of the cell* was calculated as previously described [27],

$$\text{roundness} = \frac{4\pi \times \text{area}}{\text{perimeter}^2},$$

resulting in a value between 0 and 1 where 1 represents a perfectly circular cell shape.

2.6.2 *Reorganisation of adsorbed fibronectin*

The ability of MG-63 cells to reorganise adsorbed FN (i.e., early matrix) was monitored by coating all samples with FITC-labelled FN (40 µg/ml) for 30 min at 37°C, then rinsing twice with PBS, before seeding with 2.0×10^4 cells/well in medium containing 10% FBS. After 4 h of incubation the samples were fixed using 3% paraformaldehyde, mounted in Mowiol (Sigma) and then viewed and photographed as described in Sect. 2.6.1 taking into account the specific wavelengths for FITC (excitation 492 nm and emission 518 nm). As a positive control a regular round shaped glass coverslip was used (Menzel GmbH, 15 mm diameter).

2.6.3 *Fibronectin matrix formation*

The ability of MG-63 cells to secrete and deposit FN into the extracellular matrix fibrils (i.e., late matrix) was examined via immunofluorescence. For that 3.0×10^4 cells/well were

cultured for 5 days in serum containing medium. The medium was exchanged every second day, and at the end of incubation the cells were rinsed three times with PBS before fixed with 3% paraformaldehyde for 5 min. The samples were then rinsed with PBS and saturated with 1% bovine serum albumin (BSA) for 15 min. Subsequently the samples were incubated for 30 min with a polyclonal rabbit anti-FN antibody (Santa Cruz Inc.) dissolved in 1% BSA in PBS, before stained with a goat anti-rabbit Cy3-conjugated secondary antibody (excitation 550 nm and emission 570 nm) for 30 min, and finally washed and mounted with Mowiol. The deposited FN was viewed and photographed as described in Sect. 2.6.1 but now using the red channel of the fluorescent microscope.

2.6.4 Cell proliferation

A commercially available colorimetric immunoassay based on the measurement of BrdU incorporation during DNA synthesis (Roche Applied Science) was used to evaluate the cell cycle progression after 24 h of incubation. For this purpose, non-coated samples were seeded with 6.0×10^4 cells/well in serum containing medium.

Additionally, adherent cells from three samples of each chemistry were enzymatically released after 24 h of incubation with trypsin-EDTA for 5 min at 37°C, and counted with a haemocytometer. Furthermore representative pictures of the cells viewed by FDA were taken according to Sect. 2.6.1 after 3 and 5 days in culture respectively (using a cell seeding concentration of 1.5×10^4 cells/well).

2.6.5 Cell differentiation

To quantify the level of cell differentiation we measured the alkaline phosphatase activity as well as the amount of produced osteocalcin. Samples were seeded with 1.5×10^4 cells/well in serum containing medium which was exchanged every second day. After 5 days in culture the cells had grown to confluence, and the samples were moved to a new culture plate to avoid interference from cells growing outside the sample in the culture well. From this time point, the culture medium was without serum but supplemented with sterile filtered 0.1% BSA (Sigma) and 100 ng/ml vitamin C. Also, 10 µl of vitamin D (10^{-8} M) was added to one set of samples as an additional stimulant for bone differentiation. The vitamins were continually supplemented to the culture medium every day until the end of experiment (in total 8 days in culture). Additionally, adherent cells on three samples of each chemistry were enzymatically released according to Sect. 2.6.4, and counted with a haemocytometer.

Alkaline phosphatase activity The retention of osteoblastic phenotype was partly evaluated by measuring alkaline phosphatase activity. A colorimetric method based on the conversion of *p*-nitrophenyl phosphate into *p*-nitrophenol in the presence of alkaline phosphatase was used. After eight days in culture the cells were carefully washed with PBS, and then lysed with a minimum amount of M-PER Mammalian Protein Extraction Reagent (Pierce) during 5 min. The lysed cells were stored at −80°C and after a repeated process of thawing and re-freezing the M-PER solution was mixed with 2-Amino-2-methyl-1-propanol buffer (Sigma Diagnostics Inc.) and phosphatase substrate solution (Sigma, 4 mg/ml), and incubated at 37°C for 60 min. The reaction was stopped with 3 M NaOH and the production of *p*-nitrophenol was determined by measuring the absorbance at 405 nm. The values were calibrated against a standard curve prepared from known concentrations of *p*-nitrophenol (Sigma) and then normalised to the number of cells on each sample.

Osteocalcin In parallel with evaluating the alkaline phosphates activity after 8 days in culture, also the supernatant of the cell culture was harvested. The supernatant was used to quantify the amount of produced osteocalcin using a competitive immunoassay kit (Metra^{TM} Osteocalcin EIA kit, Quidel). Absorbance was read at 405 nm with a microplate reader (PowerWave, BIO-TEK Instruments Inc.) and calibrated against a standard curve of known osteocalcin concentrations. The results were normalised to the number of cells on each sample.

2.7 Statistics

All the cell experiments were performed with at least three replicates. To quantify the cell morphology, between 270 and 642 individual cells obtained from at least five representative picture of each surface were digitally analysed. The contact angles (three triplicates for each chemistry and 11 readings for each were performed) and cell morphological parameters were quantified with GraphPad InStat 3.06 (GraphPad Software) using the non-parametric Kruskal-Wallis model followed by Dunn's post test. Other experiments were subject to ANOVA testing ($P < 0.05$). Results are presented as mean ± standard deviation.

3 Results

3.1 Surface characterisation

Besides providing distinct surface chemistries, the involved chemistries also provided a range of surface wettabillity. The measured water contact angles of SAMs and Si_3N_4

Table 1 The advancing and receding contact angles were measured for the involved chemistries. The contact angle on the COOH surface was statistically lower than the contact angle on Si_3N_4 and NH_2

Substrate	Advancing	Receding
Si_3N_4	61.5 ± 6.0	50.3 ± 3.2
NH_2	68.7 ± 4.1	58.0 ± 3.4
COOH	36.4 ± 3.0	27.9 ± 2.0

surface are presented in Table 1. The significantly lowest advancing and receding contact angle were obtained for the COOH surface followed by the Si_3N_4 and the NH_2, which did not differ significantly between each other.

3.2 Initial cellular interactions

When cells were enzymatically released after 24 h using trypsin-EDTA to measure the initial amount of osteoblasts that were adhered on the surfaces, most cells were counted from the control (TCPS) but closely followed by NH_2. The cell yield from both COOH and Si_3N_4 surfaces was significantly less (Fig. 1). The same trend was observed when quantifying BrdU-labelled DNA of proliferating cells, but by normalising the absorbance of BrdU labelled DNA to cell numbers we could evaluate the substratum specificity for initial cell growth. Then we observed that it was the COOH functionality that tended to promote initial cell proliferation (Fig. 2).

3.3 Effect of fibronectin

To better characterise the initial cellular interactions we studied the effect of FN which is the major adhesive protein in biological fluids.

3.3.1 Fibronectin adsorption

The quantity of dissolved FITC-labelled FN from each sample was determined by comparison to a standard curve prepared from labelled protein solutions. All samples provided a detectable fluorescent signal, and in all three experiments the highest fluorescent intensity was obtained from the NH_2 surface followed by the COOH, and finally the Si_3N_4 (Fig. 3).

3.3.2 Initial cell adhesion and spreading—morphological quantitative examination

The overall cell morphology on non-coated substrates after 2 h of incubation in serum free medium is shown in Fig. 4

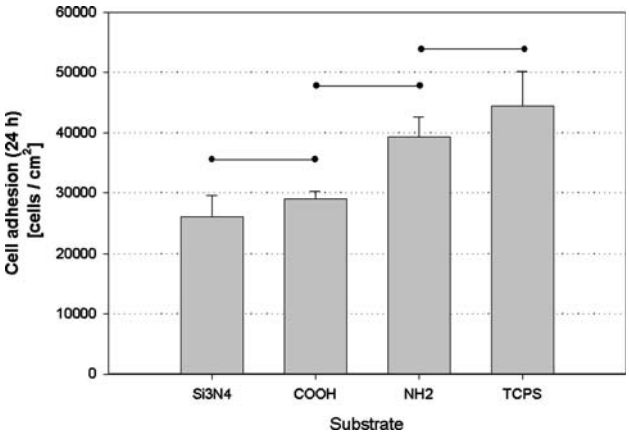

Fig. 1 Cell adhesion was quantified after 24 h of incubation by release of attached cells using trypsin-EDTA. Bars not connected with horizontal lines are statistically different ($P < 0.05$)

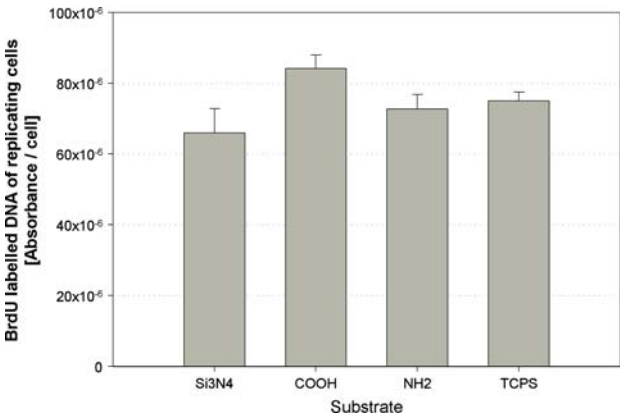

Fig. 2 Initial cell proliferation at 24 h of incubation was colourimetrically quantified through BrdU labelled newly synthesized DNA of replicating cells. The absorbance value was normalised to number of cells giving surface specific interaction in the sense that the proliferation rate for each surface could be determined

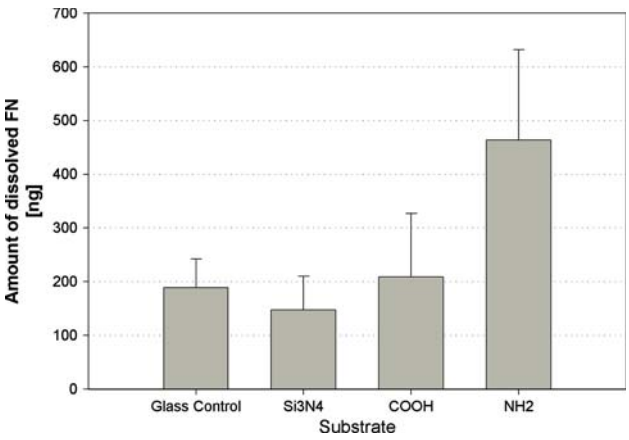

Fig. 3 FN adsorption to each surface was measured as fluorescence intensity of dissolved FITC-labelled fibronectin, and calibrated against a standard curve of known protein concentrations

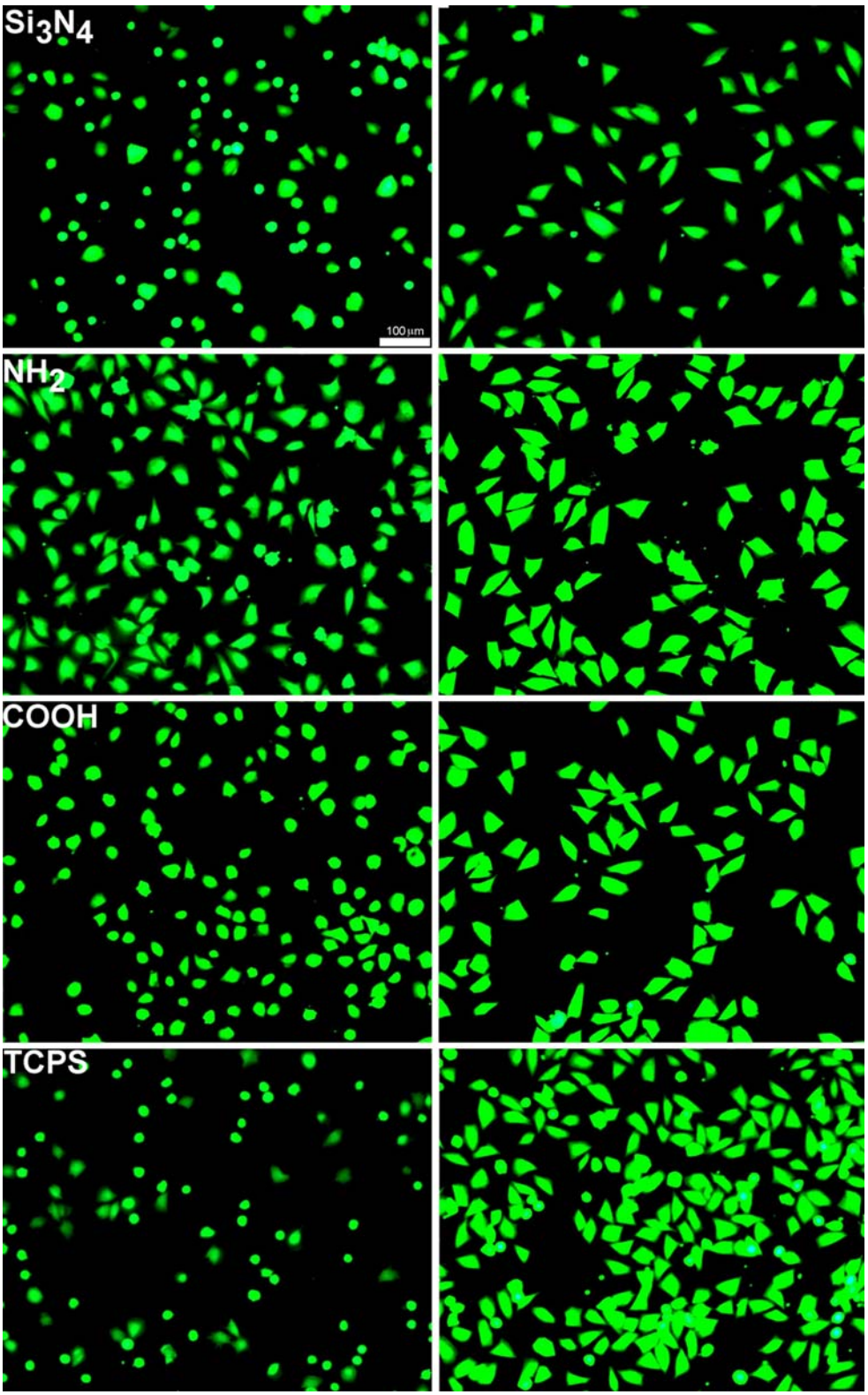

Fig. 4 Cell morphology was evaluated by staining with FDA after 2 h of incubation in serum free culture medium. The left column shows cells on non-coated samples, while the right column represents FN coated substrates

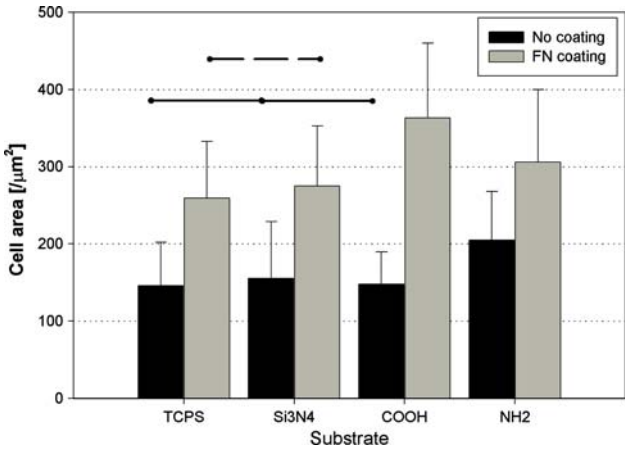

Fig. 5 The area of individual cells attached to non-coated and FN-coated substrates was quantified using FDA stained cells and image analysis software. Bars not connected with same style horizontal lines are statistically different ($P < 0.05$)

Table 2 The roundness of individual cells attached to non-coated and FN-coated substrates was calculated, resulting in a value between 0 and 1. A perfect circular cell has a value equal to 1

	Si_3N_4	COOH	NH_2	TCPS
No coating	0.54 ± 0.21	0.52 ± 0.15	0.35 ± 0.12	0.52 ± 0.14
FN coating	0.31 ± 0.09	0.27 ± 0.09	0.34 ± 0.11	0.27 ± 0.11

(left column). It could be observed that adhesion, cell area, and cell shape differed between the chemistries. On non-coated surfaces the largest cells were observed on the NH_2 (Fig. 5), while cells on Si_3N_4 and COOH were significantly smaller but did not differ from the positive control tissue culture polystyrene (TCPS). While non-coated NH_2 allowed for spontaneous spreading (roundness = 0.35) non-coated Si_3N_4 provided similar conditions for spreading (roundness = 0.53) as TCPS and COOH. The shape of cells on both TCPS and COOH were however more uniform than on Si_3N_4, which actually held a mixture of both very spread and very round cells. When the samples were coated with FN (Fig. 4 right column and Fig. 5) a significant increase in cell area was observed on all samples but with the greatest response on the COOH chemistry (146% of increase). Also the roundness of cells was greatly affected by FN coating (Table 2).

3.3.3 Reorganisation of adsorbed fibronectin

The ability of MG-63 cells to remove and reorganise adsorbed FITC-labelled FN after 4 h of incubation (early matrix) was present only on the COOH chemistry and on the positive control glass, while on both Si_3N_4 and NH_2 the pre-adsorbed FN layer was left completely intact (Fig. 6, left column).

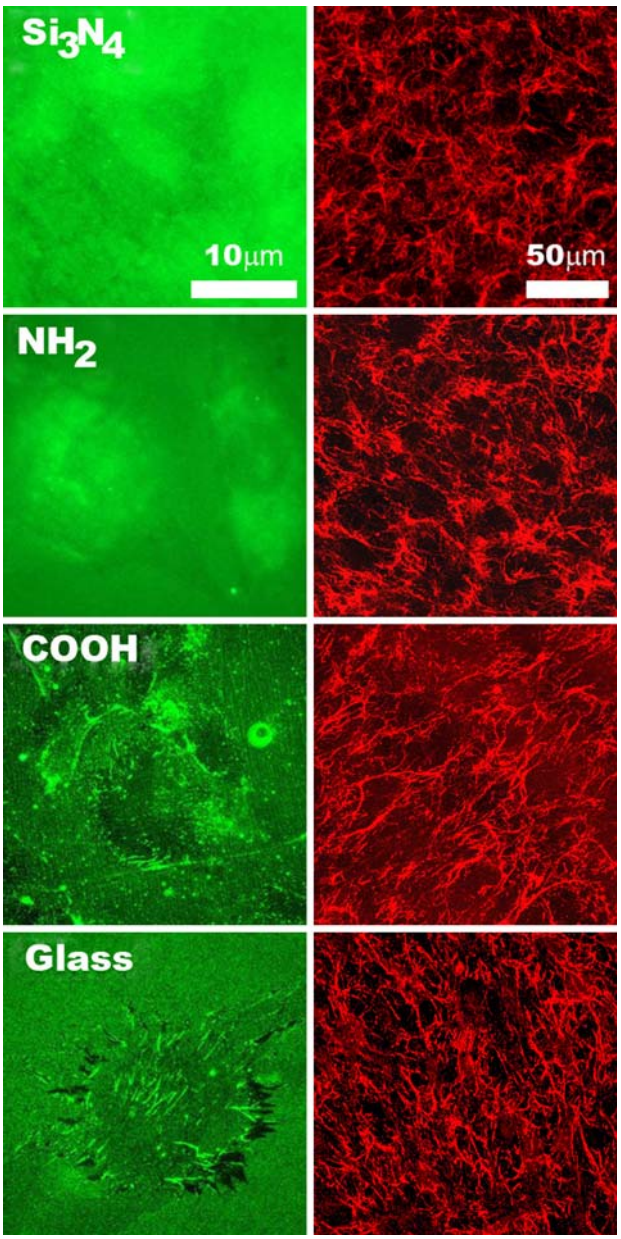

Fig. 6 Removal and reorganisation of pre-adsorbed FITC-labelled FN (ex 492 nm, em 518 nm) by cells cultured for 4 h in serum containing medium was present only on the COOH chemistry and the glass control (left column). The spatial organisation of extracellular FN produced by the cells after 5 days in culture was obtained from immunofluorescense (ex 550 nm, em 570 nm) and observed to be similar on all chemistries (right column)

3.4 Functional response of osteoblasts

3.4.1 Proliferation response

When measuring the amount of cells after eight days of incubation we found that MG-63 cells grew very well on all surfaces, but particularly on NH_2 (Fig. 7). A statistically non-significant tendency for less cell growth was measured

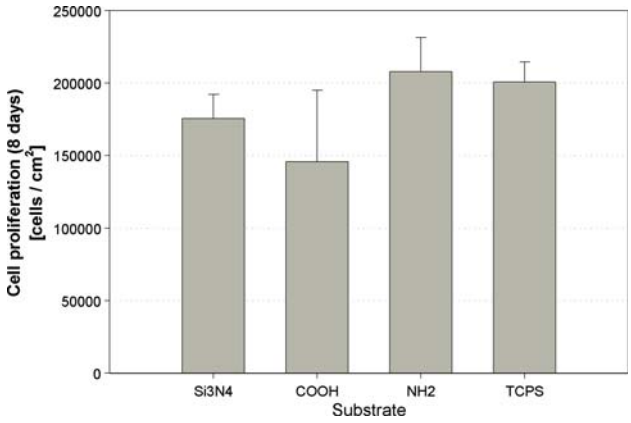

Fig. 7 Cell proliferation after 8 days of incubation was quantified with a haemocytometer after release of attached cells using trypsin-EDTA

on the COOH functionality, while Si_3N_4 represented intermediate proliferation close to the TCPS control. Morphological information on cell proliferation was obtained from the representative pictures of FDA stained cells that were taken after 3 and 5 days in culture (Fig. 8). Before reaching confluence one could observe a different pattern of cell organisation as cells on Si_3N_4 more often grew in aggregates. Towards the end of the incubation all surfaces provided overconfluent layers of cells.

3.4.2 Organisation of cell layer and matrix deposition

When overconfluent the osteoblasts grew in a film-like structure that served as a rather three-dimensional environment, and which made them less dependent of the substrate. While this film-like structure was observed to be very well attached on NH_2, and somewhat less strongly to COOH, it was very loosely associated with the Si_3N_4 surface and was easily removed by washing or changing the medium. Conversely the spatial organisation of FN matrix that was produced by the cells after 5 days in culture did not show much difference between the surfaces (Fig. 6, right column). The osteoblasts generally deposited FN fibrils in a facet-like pattern following the specific organisation of cell layer.

3.4.3 Alkaline phosphatase activity

The phenotypic expression of cells after eight days in culture was evaluated through a colorimetric analysis for alkaline phosphatase activity (Fig. 9). Spontaneous alkaline phosphatase activity was observed on all substrates. After normalisation to cell number the highest activity was observed on TCPS, closely followed by COOH and Si_3N_4, and finally by NH_2 where the activity was significantly less than on all other surfaces. The addition of vitamin D resulted in significantly higher alkaline phosphatase activity on all substrates.

3.4.4 Osteocalcin expression

The expression of osteocalcin by MG-63 cells was analyzed by ELISA (Fig. 10). Spontaneous production of osteocalcin was only detected from cells cultured on the Si_3N_4. When the cell culture medium was supplemented with vitamin D the level of osteocalcin was substantially increased on all chemistries but without any significant differences between the different substrates.

4 Discussion

The very first link in a chain of events that determines the biocompatibility of a surface is the protein adsorption. It is not only the adsorbed quantity, but also the protein conformation and its binding strength to the surface that will determine future cell behaviour. It is further well known that protein adsorption and subsequent cell adhesion to a material depend on both surface chemistry and surface wettability [28], where the latter parameter in this study ranged from very hydrophilic (COOH) to intermediate hydrophobic (NH_2). The Si_3N_4 surface which exposes a mixture of OH– and NH_2–groups [29] was as previously reported also intermediate hydrophobic [13]. The FN adsorption to our model surfaces varied as $NH_2 >$ COOH $>$ Si_3N_4, but the cell spreading on FN-coated substrates was equally pronounced on all substrates indicating proper protein conformation. Eventhough we cannot exclude different surface densities of our SAMs, our protein adsorption results confirm earlier studies claiming that the NH_2 chemistry binds more FN than the negatively charged COOH at physiological pH [30, 31], and also show that FN adsorption is predominated by surface chemistry rather than surface wettability in this specific case. The observed high spontaneous cell spreading on non-coated NH_2 chemistry was probably due to a combination of increased adsorption of adhesive proteins that always exist as traces in the medium, and from the fact that the cells could easily overcome the electrostatic barrier—effects that could promote both faster cell adhesion and higher cell spreading.

It is also important to note that the adsorbed protein layer is not a static environment but can be extensively remodelled by cells [32]. For example, one of us earlier demonstrated that fibroblasts can arrange FN on hydrophilic glass but not on hydrophobic octadecylsilane surface

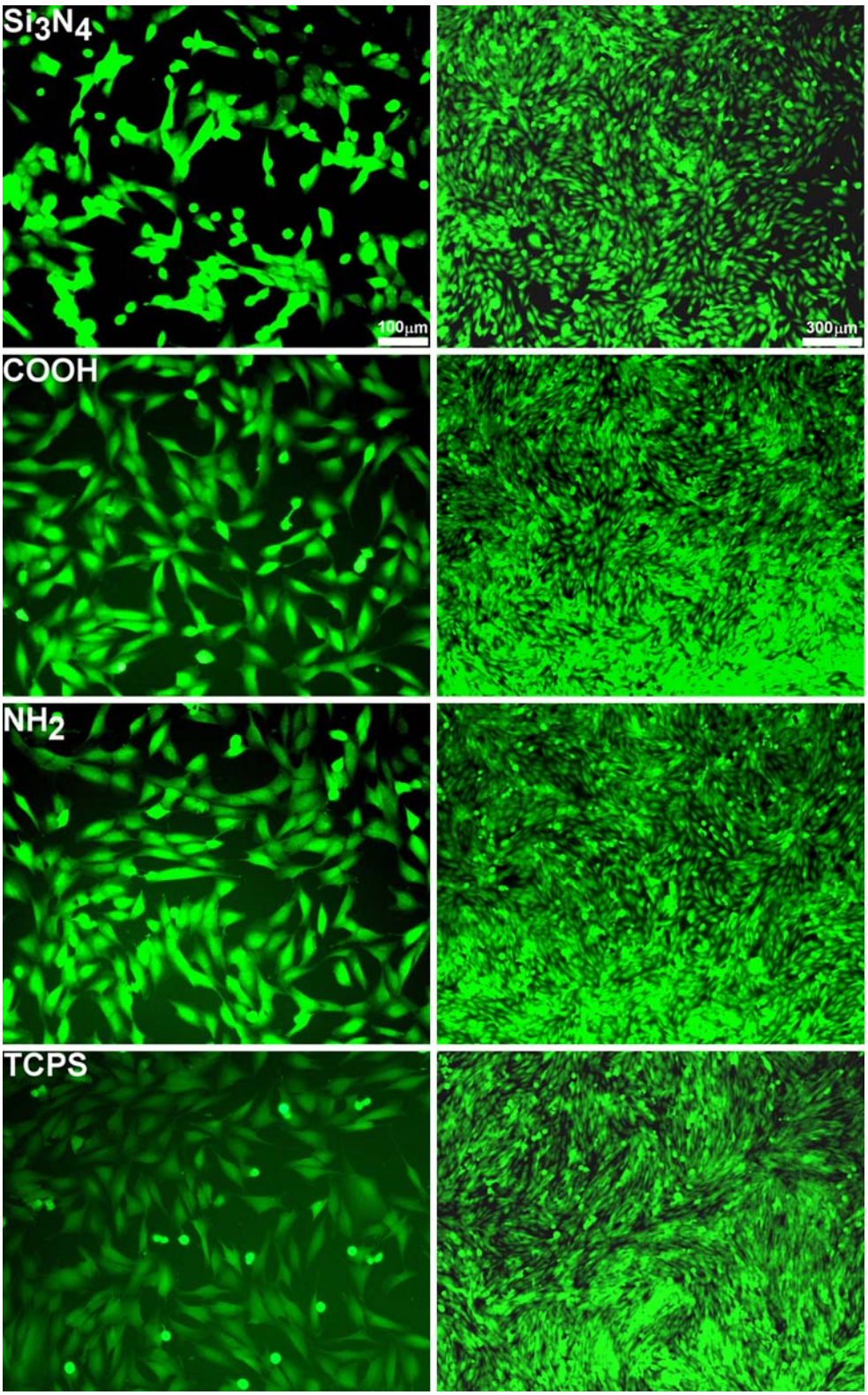

Fig. 8 Representative pictures of cells stained with FDA after 3 days in culture (left column) and five days in culture (right column). Cluster-like cell growth was often observed on the Si_3N_4 substrate before confluence was reached

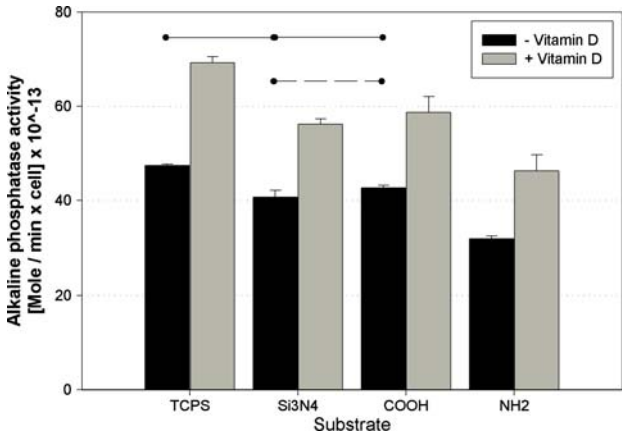

Fig. 9 Detected level of alkaline phosphatase activity from cells was normalised to cell number. Bars not connected with horizontal lines are statistically different ($P < 0.05$)

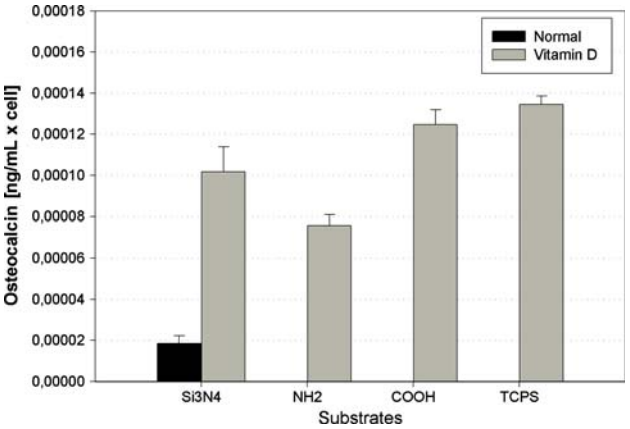

Fig. 10 Detected level of osteocalcin was normalised to cell number. Without adding vitamin D to the culture medium production of osteocalcin was only detected from cells cultured on Si_3N_4

[18]. Such inability of attached cells to actively remove and reorganise adsorbed FN can thus be considered as an indirect measure on high binding strength between the protein and the surface. In this study we observed that the osteoblast-like MG-63 cells were able to remove and reorganise pre-adsorbed FN from both hydrophilic glass and COOH functionality. This is in fact in accordance with literature as it has previously been reported that COOH chemistry promote fibroblast FN reorganisation while NH_2 chemistry does not [26]. Here we show the same response but with osteoblast-like cells and speculate that absent FN reorganisation on Si_3N_4 and NH_2 is due to higher binding strength between the protein and these two surfaces than to the negatively charged COOH. As it has previously been shown that the process of interfacial FN reorganisation also could play an important role for materials biocompatibility [18], here is the place to mention that the COOH functionality was observed to promote the initial proliferation of osteoblasts.

When cells were left for longer times they proliferated well on all samples, and particularly on the NH_2 chemistry. It was also observed that on all substrates the osteoblasts were preferably growing within their newly secreted gel-like matrix which became well organised and dense, presumably because of the development of intermolecular cross-links. As a result it behaved as an entire tissue-like structure rather than a single cellular layer that is more dependent on the underlying surface chemistry. This film-like structure was furthermore easily detached from the Si_3N_4 by regular washing forces, indicating low attachment strength. Conversely, on the positively charged NH_2 the cell layer adhered more strongly and could not be removed even after extensive flushing with medium. Negatively charged COOH substrate represented an intermediate resistance to flushing but still bound well the cell layer. It is well documented that the early osteoblasts matrix consists of type I collagen and various bone specific glucosaminoglycans [33], but it is also enriched with FN fibrils, a fact that we confirm in this study. It has however not been well described how osteoblasts spatially organise newly synthesized FN. Here we found that their FN matrix is arranged in a specific facet-like pattern, very distinct from the FN secreted by fibroblasts that is usually linearly organised. We speculate that the face-like arrangement of FN could support, or even serve as a template for the future organisation of osteoblasts in the alveolar structures, a specific morphological feature of their differentiation in three dimensions. We also show that the organisation of this FN did not differ between various surfaces, which mean that the underlying chemistry not anymore influenced the ability of osteoblasts to organise their matrix. Thus we anticipate that in a distinct moment of osteoblasts matrix development the intermolecular binding strength between matrix components will override the protein substratum interaction, which may result in its sequestration from the surface, particularly upon application of a distinct external force. This is partly confirmed via immunofluorescence by the fact that we could not detect neither FN nor type I collagen left on the substratum after the tissue-like film was flushed away from the different chemistries (data not shown). Nevertheless we concluded that the observed stronger interaction of this matrix, particularly with NH_2, followed by COOH functionality will positively influence the osseointegration, i.e. the process by which mature bone is deposited directly on implant materials without any intervening soft or fibrous tissue [34]. One can also consider the loosely attached tissue-like structure on Si_3N_4 to partly be a consequence of the promoted intercellular (homotypic) interactions frequently observed during subconfluent cell growth.

The main event in tissue repair and regeneration is the ability of cells to restore the functionality of damaged tissue. Therefore osteoblasts differentiation is of greatest relevance for the evaluation of future osseointegration. In this study we followed the differentiation by quantifying two well known markers for bone formation, alkaline phosphatase activity (early marker) and secretion of osteocalcin (late marker). Our main conclusions were that both spontaneous and stimulated alkaline phosphatase activities were reduced on the NH_2 compared to the other chemistries, and that Si_3N_4 promoted cells to earlier go into a mature stage (as seen by spontaneous osteocalcin production). It has to be admitted however that it previously [35] has been stated that NH_2 promotes alkaline phosphatase activity and osteocalcin production to a higher extent than COOH, a contradictory result to ours. In that study however, the SAMs were coated with FN and thereby they eliminated possible differences in the initial cell adhesion. We speculate that on non-coated surface, as in our study, the cells have to "rely" more on their own production and organisation of matrix, where they may behave differently. Nevertheless, we believe that the initial cell adhesion might influence the later cell differentiation. There are indications in literature that NH_2 binds cells much more strongly than COOH [21], presumably due to electrostatic interaction between the positively charged surface and the negatively charged cell surface. Thus, from our observations it might be speculated that a strong substratum interaction of both cells and their matrix, logically considered as positive event for osseointegration, may disturb the proper osteoblasts differentiation on certain materials interfaces. Further studies are now on the way to confirm or to exclude this possibility.

5 Conclusions

Considering ISFET applications we suggest that Si_3N_4 has an appropriate biocompatibility for osteoblast-like MG-63 cells. The low protein adsorption to Si_3N_4 vouches for prevented biofouling while cells are still able to proliferate and differentiate very well. Furthermore, the loose cellular and matrix interactions with the underlying surface should facilitate the detection of protons helping to maintain the sensitivity of the ISFET sensor. However, when the aim is to monitor cell growth using electrical impedance spectroscopy one should consider a surface chemistry that promotes the osseointegration more than Si_3N_4 does. We show that certain SAMs on Si_3N_4 effectively enhance the tissue integration. Since the COOH chemistry has a modest FN adsorption while cells are well attached, proliferate and differentiate well we suggest this surface chemistry a proper choice for EIS measurements.

Acknowledgements This work was part of the European funded project NMP3-CT-2005-013912. The authors thank Drs. F. Bessueille and M. Pla-Roca of the Barcelona Science Park for help with the silanisation. J.G. acknowledges support from the Catalonian Government, Grant (2006FI00863), and Folke y Margit Pehrzon foundation. G.A acknowledges grants AGAUR 2004PIV25 from the Catalonian Government and SAB2004-0209 from the Spanish Ministry of Education and Science. E.E. acknowledges the Spanish Ministry of Education and Science for the Juan de la Cierva Grant. Roche Diagnostics is acknowledged for the provided vitamin D.

References

1. R. Kue, A. Sohrabi, D. Nagle, C. Frondoza, D. Hungerford, Biomaterials **20**, 1195 (1999)
2. A. Sohrabi, C. Holland, R. Kue, D. Nagle, D.S. Hungerford, C.G. Frondoza, J. Biomed. Mater. Res. **50**, 43 (2000)
3. A. Neumann, T. Reske, M. Held, K. Jahnke, C. Ragoß, H.R. Maier, J. Mater. Sci. Mater. Med. **15**, 1135 (2004)
4. P. Bergveld, Sensor. Actuat. B-Chem. **88**, 1 (2003)
5. M.J. Schöning, M. Thust, M. Müller-Veggian, P. Kordoš, H. Lüth, Sensor. Actuat. B-Chem. **47**, 225 (1998)
6. W.H. Baumann, M. Lehmann, A. Schwinde, R. Ehret, M. Brischwein, B. Wolf, Sensor. Actuat. B-Chem. **55**, 77 (1999)
7. S. Mohri, J. Shimizu, N. Goda, T. Miyasaka, A. Fujita, M. Nakamura, F. Kajiya, Sensor. Actuat. B-Chem. **115**, 519 (2006)
8. P. Clechet, Sensor. Actuat. B-Chem. **4**, 53 (1991)
9. A. Tlili, M.A. Jarbour, A. Abdelghani, D.M. Fathalah, M.A. Maaref, Mater. Sci. Eng. C **25**, 490 (2005)
10. S. Roy, A.J. Fleischman, Sensor. Mater. **15**, 335 (2003)
11. P.R. Hernández, C. Taboada, L. Leija v. Tsutsumi, B. Vázquez, F. Valdés-Perezgasga, J.L. Reyes, Sensor. Actuat. B-Chem. **46**, 133 (1998)
12. G. Voskerician, M.S. Shive, R.S. Shawgo, H. von Recum, J.M. Anderson, M.J. Cima, R. Langer, Biomaterials **24**, 1959 (2003)
13. C.S. Giannoulis, T.A. Desai, J. Mater. Sci. Mater. Med. **13**, 75 (2002)
14. N. Wisniewski, M. Reichert, Colloids Surf. B **18**, 197 (2000)
15. R. Gifford, J.J. Kehoe, S.L. Barnes, B.A. Kornilayev, M.A. Alterman, G.S. Wilson, Biomaterials **27**, 2587 (2006)
16. R. Hynes, *Fibronectins*. (Springer-Verlag, New York, 1990)
17. G. Altankov, F. Grinnell, T. Groth, J. Biomed. Mater. Res. **30**, 385 (1996)
18. G. Altankov, T. Groth, J. Mater. Sci. Mater. Med. **5**, 732 (1994)
19. R. Tzoneva, T. Groth, G. Altankov, D. Paul, J. Mater. Sci. Mater. Med. **13**, 1235 (2002)
20. N. Faucheux, R. Schweiss, K. Lützow, C. Werner, T. Groth, Biomaterials **25**, 2721 (2004)
21. M. Lee, D. Brass, R. Morris, R. Composto, P. Ducheyne, Biomaterials **26**, 1721 (2005)
22. M. Veiseh, M. Hadi Zareie, M. Zhang, Langmuir **18**, 6671 (2002)
23. I. Marques de Oliverira, M. Pla, L.I. Escriche, J. Casabó, N. Zine, J. Bausells, F. Bessueille, J. Samitier, A. Errachid, Proc. IEEE Sensors. **2**, 726 (2004)
24. M. Bras, V. Dugas, F. Bessueille, J.P. Cloarec, J.R. Martin, M. Cabrera, J.P. Chauveti, E. Souteyrand, M. Garrigues, Biosens. Bioelectron. **20**, 797 (2004)
25. M. Riedel, B. Müller, E. Wintermantel, Biomaterials **22**, 2307 (2001)
26. N. Faucheux, R. Tzoneva, M-D. Nagel, T. Groth, Biomaterials **27**, 234 (2006)
27. M. Bergkvist, J. Carlsson, S. Oscarsson, J. Biomed. Mater. Res. Part A **64A**, 349 (2003)

28. C.J. Wilson, R.E. Clegg, D.I. Leavesley, M.J. Pearcy, Tissue Eng. **11**, 1 (2005)
29. M. Yuqing, G. Jianguo, C. Jianrong, Biotechnol. Adv. **21**, 527 (2003)
30. B.G. Keselowsky, D.M. Collard, A.J. García, J. Biomed. Mater. Res. Part A **66A**, 247 (2003)
31. M.H. Lee, P. Ducheyne, L. Lynch, D. Boettiger, R.J. Composto, Biomaterials **27**, 1907 (2006)
32. P. Sivakumar, A. Czirok, B.J. Rongish, V.P. Divakara, Y.P. Wang, S.L. Dallas, J. Cell Sci. **119**, 1350 (2006)
33. J. Termine, P. Gehron Robey, in *Primer on the Metabolic Bone Diseases and Disorders of Mineral Metabolism*, Ed. by M. Favus, (Lippencott-Raven Publishers, Philadelphia, 1996) p 24
34. M. Ahmad, M. McCarthy, G. Gronowicz, Biomaterials **20**, 211 (1999)
35. B.G. Keselowsky, D.M. Collard, A.J. García, Proc. Natl. Acad. Sci. USA **102**, 5953 (2005)